

SCIENTIFIC REPORTS



OPEN

The effects of magnetic fields exposure on relative permittivity of saline solutions measured by a high resolution SPR system

Received: 08 January 2016

Accepted: 11 April 2016

Published: 28 April 2016

Li Jiang^{1,*}, Xinyuan Zhao^{2,*}, Yue Fei², Dongdong Yu², Jun Qian¹, Jinguang Tong¹, Guangdi Chen² & Sailing He¹

A measurement system for the relative permittivity of a physiological solution under 50 Hz magnetic fields (MF) is presented. It is based on a phase-sensitive surface plasmon resonance (SPR) system. Relative permittivity was analyzed for different solute concentrations of sodium chloride under various MF exposure parameters. We found that MF exposure at 0.2–4.0 mT step-wise decreased significantly the SPR phase signal of a 0.9% sodium chloride solution while 0.1 mT of MF exposure did not. The decreases in the SPR phase signal depended on the duration of MF exposure, and the signal reached a plateau after 15 min of exposure. Interestingly, the decreased SPR phase signal showed a gradual increase and approached the background level when the exposure was drawn off. In addition, we found that the response of the sodium chloride solution to MF also depended on its concentration. In brief, the relative permittivity of sodium chloride in solutions appears to be practically affected by 50 Hz MF exposure. Our data indicates that the relative permittivity of the saline solution influenced by MF exposure should be considered when investigating the biological effects of MF exposure on organisms in experimental study.

With the development of the electric power industry and wide usage of electronic products, the public concerns have been raised on exposure to increasing electromagnetic fields, especially extremely low frequency magnetic fields (ELF-MF), which range from 1–300 Hz. In 2002, the International Agency for Research on Cancer (IARC) has classified ELF-MF as a possible carcinogen to humans according to limited epidemiological evidences¹. It remains inconclusive whether exposure to ELF-MF increases risks of other detrimental health effects². Moreover, laboratory studies did not clarify the biological effects induced by ELF-MF and their underlying mechanisms^{3–5}. The critical issue is that the biophysical mechanisms of ELF-MF acting on organisms are not clear.

Dielectric properties are vital biophysical features of biological tissues, and biological activity is an index to assess the active state of tissues. Wang *et al.* has reported that the dielectric properties of human tissue are related to its biological activities⁶. The permittivity, which is a vital dielectric property related to the ability to store electric charge, has a great value in various medical areas including electromagnetic protection, electromagnetic imaging, and disease diagnosis^{7–9}. Thus, it is reasonable that the normal dielectric properties of tissues or cells are important for maintaining their biological function. It is well known that permittivity is related to refractive index. For the saline solution, a non-magnetic material, μ_r is very close to 1, thus, we can obtain $n = \sqrt{\epsilon_r}$, where ϵ_r represents the relative permittivity and n represents the refractive index^{10,11}. To that end, we studied the effects of ELF-MF exposure on refractive index with phase-interrogation surface plasmon resonance (SPR) sensing.

Surface plasmons are free electron oscillations at the metal-dielectric interface and can be optically excited¹². SPR sensing is an optical refractive index sensing technology with high sensitivity, label-free and real-time detection¹³. It has been widely applied in many areas, including proteomics, pharmacy, genomics, pollutants

¹State Key Laboratory of Modern Optical Instrumentation (Zhejiang University), Centre for Optical and Electromagnetics Research, Zhejiang Provincial Key Laboratory for Sensing Technologies, JORCEP (Sino-Swedish Joint Research Center of Photonics), Zhejiang University, Hangzhou 310058, China. ²Bioelectromagnetics Laboratory, Zhejiang University School of Medicine, Hangzhou 310058, China. *These authors contributed equally to this work. Correspondence and requests for materials should be addressed to G.C. (email: chenguangdi@zju.edu.cn) or S.H. (email: Sailing@kth.se)

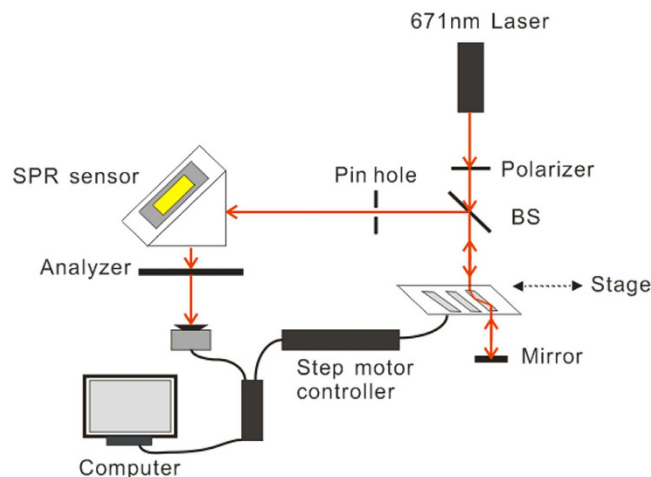


Figure 1. Schematic diagram showing the setup of phase-sensitive SPR sensing system based on PM-PPM.

detection, and food safety^{14–21}. Conventional SPR sensors are based on amplitude detection and can be classified as intensity-interrogation²², angle-interrogation²³ and wavelength-interrogation²⁴. SPR sensors based on phase-interrogation have been extensively studied since the late 1990s, because their resolution is 2 to 3 orders of magnitude higher than that of amplitude-interrogation (10^{-7} – 10^{-8} RIU)^{10,25–27}. The change in permittivity of the sample could be reflected by the SPR phase signal change. That means, when the change in SPR phase signal is detected, we can consider that the permittivity of the sample changes. In this study, we have obtained the SPR phase signals of sodium chloride solutions under ELF-MF exposure with various parameters in a phase-interrogation SPR sensing system based on a novel parallel-moving prism phase modulator (PM-PPM). The effects of ELF-MF on sodium chloride solutions with different concentrations have been studied by analyzing the changes in SPR phase signals.

Results

Figure 1 shows the setup of our phase-sensitive SPR sensing system. In this system, a stabilized laser with a wavelength of 671 nm was used as the light source. The light went through a linear polarizer and a beam splitter, and was then incident into the PM-PPM, which was equipped with three BK7 rhombic prisms. A mirror was used to reflect the light back into the prism. The modulated light was then filtered with a pin hole to reduce the stray light and struck the SPR sensor at an appropriate angle to meet the resonance condition. The reflected light from the SPR sensor passed through an analyzer, and then the interference light was detected by a photo detector. The SPR sensor in the Kretschmann configuration included a homemade microfluidic chip (size: 25.4×25.4 mm²) with one reaction chamber and one gold spot, and a right angle coupling prism.

Detection Sensitivity. To explore the detection sensitivity of SPR on the refractive index, the SPR signals of different concentrations of sodium chloride solutions were measured at a constant temperature of 25 °C, since it is well known that the refractive index of chloride solution is positively related with concentration. The results showed that the SPR signal was gradually increased following increased concentration (Fig. 2a,b). We also found that the detection limit on the concentration of SPR was lower than 0.01%, suggesting a relatively high sensitivity. SPR phase corresponding to glycerin solutions with various known refractive index values were also detected (Fig. 2c). From this we could see that the sensitivity and resolution of our system were about 1900 rad/RIU and 3.421×10^{-7} RIU (calculated using Equ. (S1) and (S2)). The curve between every two spots in Fig. 2(c) could be seen as a linear line, which could be used to estimate refractive index change of sodium chloride solutions after MF exposure (Supplementary: Table S1).

Study on the Effects of ELF-MF on the Permittivity of Sodium Chloride Solutions. By exploring the effects of ELF-MF on the relative permittivity of sodium chloride solutions, an SPR signal of 0.9% sodium chloride solution, a physiological saline solution, was measured in the presence or absence of 50 Hz MF exposure. The results demonstrated that the SPR phase signal decreased under MF exposure in a time-dependent manner when compared to the control experiment, which did not have MF exposure (Fig. 3a,b). Interestingly, the SPR phase signal reached a constant value after 15 min of MF exposure. Next, we exposed sodium chloride solutions to different exposure intensities of MF for 15 min and measured the SPR signals. We found that MF decreased SPR signals in a dose-dependent manner, and MF at as low as 0.2 mT could significantly increase the SPR signal. However, 0.1 mT of MF exposure did not show any significant change (Fig. 3c,d). To evaluate whether MF at 0.1 mT affect the SPR signal for longer exposure durations, we exposed the solution to 0.1 mT MF for a longer time, and found that none of the indicated exposure durations successfully affected the signal, indicating that 50 MF with an exposure intensity higher than 0.1 mT is necessary for initiating a response from the SPR signals (Fig. 4a,b). Taken together, these results suggested that MF exposure decreases the permittivity of sodium chloride solutions in a time and dose dependent way. One spot

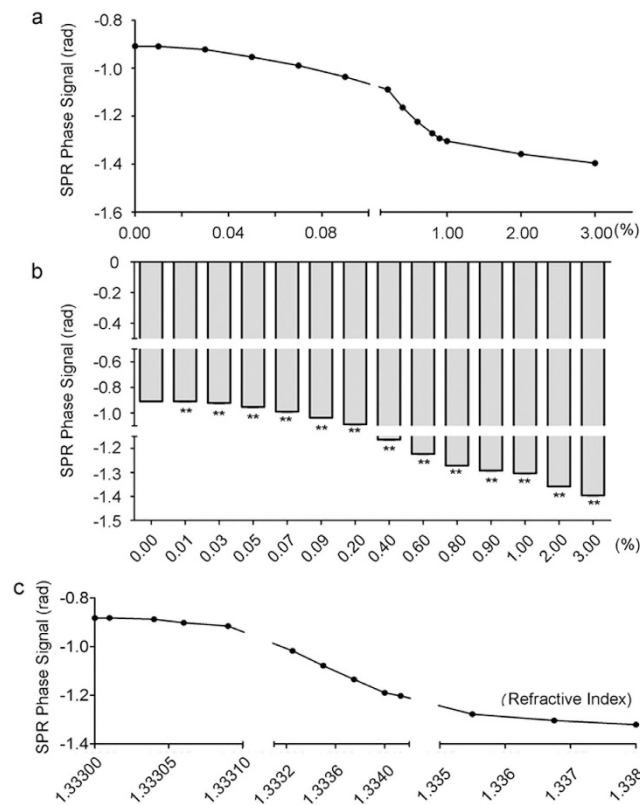


Figure 2. SPR phase signals of sodium chloride solutions with different concentrations. (a) Representative SPR phase signal curve of different concentrations of sodium chloride solutions. (b) A graph showing a statistical analysis of the SPR phase signal in different concentrations of sodium chloride solutions compared with 0.00%. All the quantitative data are presented as mean \pm SD, $**P < 0.01$. (c) SPR phase signals corresponding to glycerin solutions with different refractive index values known at the wavelength of 671 nm.

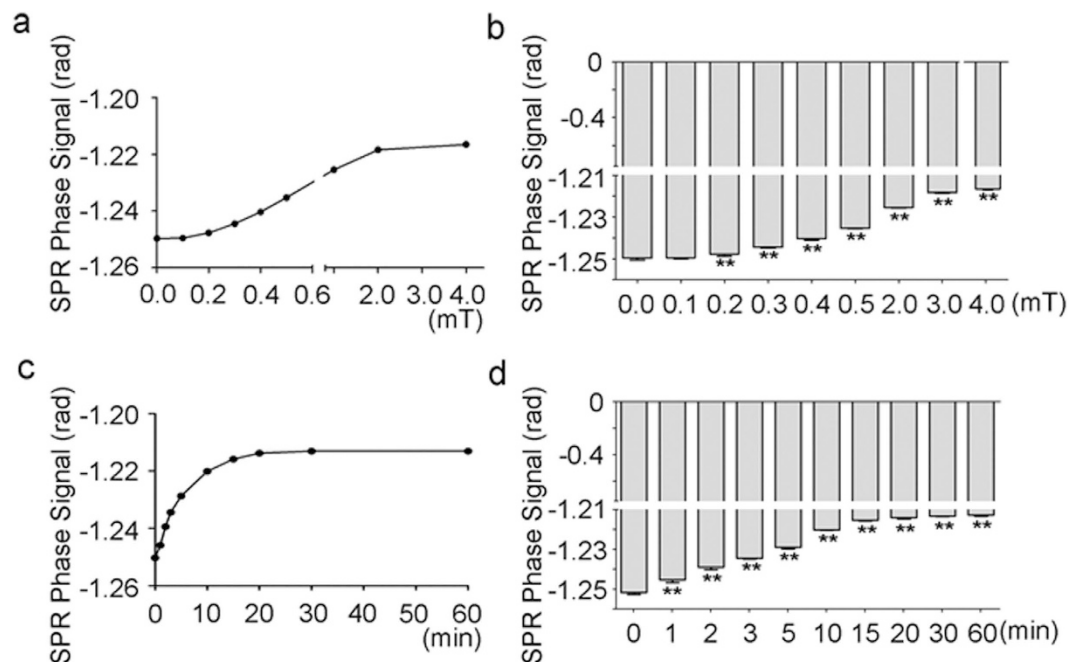


Figure 3. The effects of MF exposure on SPR signals of sodium chloride solutions. (a) MF decreased the SPR signal in a time-dependent manner. (b) A graph showing a statistical analysis for (a). (c) MF decreased the SPR signal in a dose-dependent manner. (d) A graph showing a statistical analysis for (c). All the quantitative data are presented as mean \pm SD, $**P < 0.01$ (comparing to the control of shame exposure).

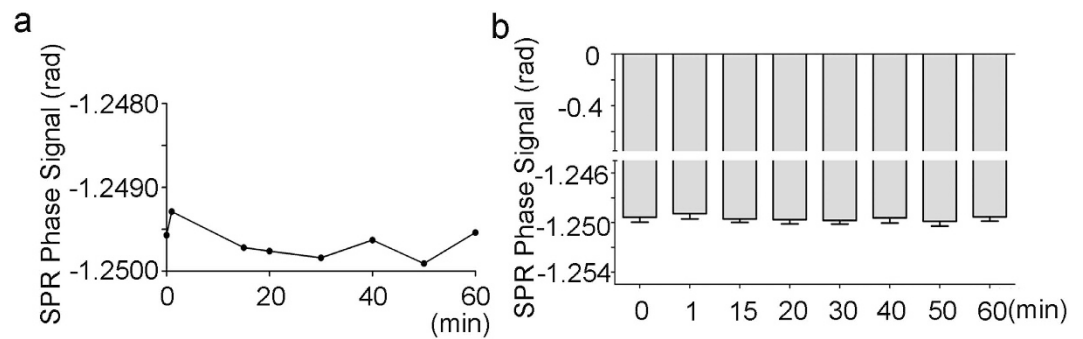


Figure 4. The effects of MF exposure at 0.1 mT on SPR signals in 0.9% sodium chloride solutions. (a) The effects of 0.1 mT MF on the SPR signals of the solution for the indicated time. (b) A graph showing a statistical analysis for (a) (compared to the control of shame exposure).

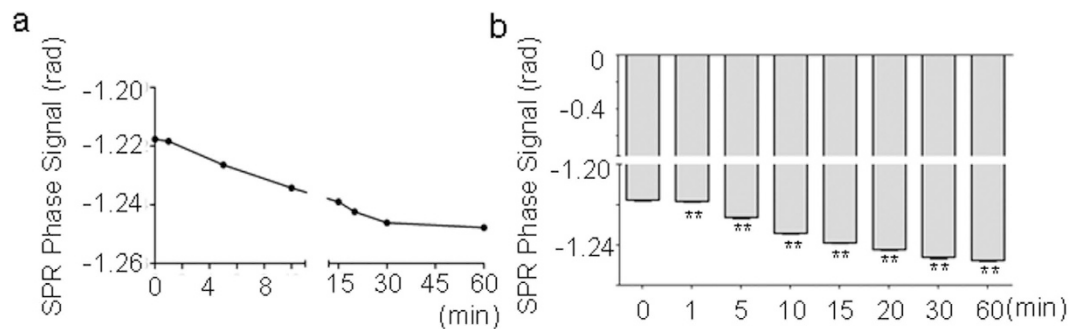


Figure 5. Recovery of SPR signals of sodium chloride solutions when the MF exposure was drawn off. (a) SPR signal (that has been decreased by MF earlier) now increases (i.e., recover) in a time-dependent way. (b) A graph showing a statistical analysis for (a). All the quantitative data are presented as mean \pm SD, ** $P < 0.01$ (comparing to the control of shame exposure).

(50 Hz, 4.0 mT, 15 min) of 0.9% sodium chloride solution was chosen to estimate the refractive index change caused by MF exposure. According to the curve between SPR phase signal and refractive index (Fig. 3c), the change was about -3.95×10^{-4} RIU (Supplementary: Table S1).

The Effects of the ELF-MF on Permittivity of Sodium Chloride Solutions is Reversible. We next evaluated if the effects of MF exposure on SPR signals in sodium chloride solutions were reversible. To that end, we exposed the solution to MF at 4.0 mT for 15 min and then had the exposure drawn off. We found that the MF-decreased SPR phase signals began to intensify immediately even only 1 minute after exposure, gradually increased during the recovery time, and almost approached the background level (before any MF exposure) after 60 min (Fig. 5a,b). These results indicate that permittivity decreased by MF is reversible.

The Effects of MF on Permittivity is Dependent on Concentration of Solutions. Since the decreases of SPR phase signals of sodium chloride solutions depend on MF exposure duration and dose, we next evaluated whether these effects depend on the solution itself, e.g., the concentrations of the solution. The SPR signals of sodium chloride solutions at 0.09%, 0.3%, 0.9% and 3% were examined. The results showed that MF exposure to 0.1 mT for 15 min was able to significantly affect the SPR signals of 3% sodium chloride solutions but not lower concentrations of solutions (Fig. 6a–c). The MF exposure threshold for a SPR signal response of the 0.09% solution was up to 0.4 mT, suggesting that a lower solution concentration of sodium chloride results in a higher responsive threshold of MF exposure (Fig. 6c). In addition, we found that the solution concentration was a critical factor for the amplitude of the decreased SPR signals. The solutions with higher concentration were more responsive to MF under the same exposure parameters (Fig. 6d). Interestingly, we found similar response of human serum to ELF-MF exposure, in which the 50 Hz at 4.0 mT could decrease the amplitude of SPR phase signal (Supplementary: Fig. S1). These results indicate that bodily fluids for organisms might respond to MF differently.

Discussion

In this study we have measured relative permittivities (refractive index) of sodium chloride solutions under 50 Hz magnetic fields based on a phase-sensitive surface plasmon resonance (SPR) system with a high sensitivity of about 1900 rad/RIU and a high resolution of about 3.421×10^{-7} RIU. We have found that SPR phase signals (monotonously related to the relative permittivity) decrease under MF exposure in a time and dose dependent

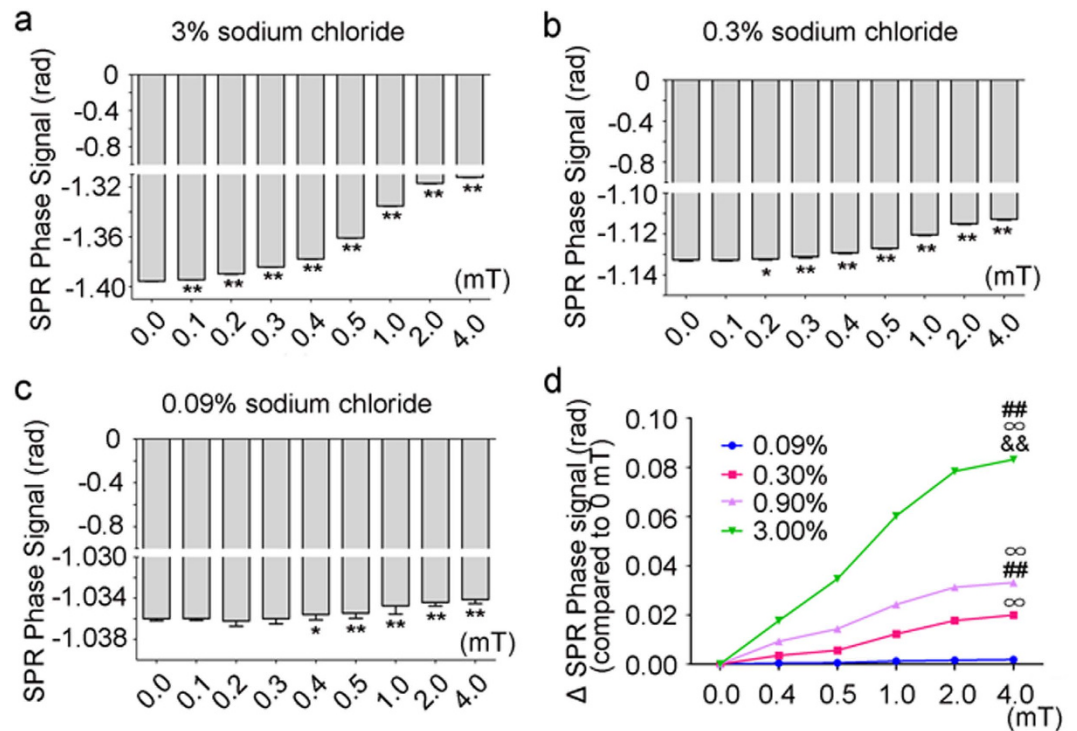


Figure 6. The effects of MF exposure on SPR signals of sodium chloride solutions with different concentrations. (a) The effects of MF of various magnitudes on a SPR signal of 3% sodium chloride solutions. (b) The effects of MF on a SPR signal of 0.3% sodium chloride solutions. (c) The effects of MF on a SPR signal of 0.09% sodium chloride solutions. (d) SPR signal responses of sodium chloride solutions with different concentrations as the magnitude of the MF exposure increases. All the quantitative data are presented as mean \pm SD, * $P < 0.05$, ** $P < 0.01$.

manner, and the decreased SPR phase signals were reversible when the exposure was drawn off. Furthermore, the SPR signal responses of sodium chloride solutions depend on the solute concentrations. For 0.9% sodium chloride solution, the refractive index decreased by 3.95×10^{-4} RIU after MF exposure (50 Hz, 4.0 mT, 15 min). Similar to 50 Hz MF exposure, we found that exposure to ELF-MF of other frequency (e.g., 30 Hz and 130 Hz) could decrease SPR phase signals in sodium chloride solutions (Supplementary: Fig. S2). Abbe refractometer was also used to measure the refractive index of 0.9% sodium chloride solution after MF exposure (Supplementary: Fig. S3), which was in good agreement with the results of SPR sensing. However, compared to abbe refractometer, SPR sensing offers higher sensitivity and resolution, which can detect much smaller refractive index change. Our data suggest that the relative permittivity of a saline solution is influenced by MF exposure, which should be considered in experimental studies on the biological effects induced by MF exposure.

It has been reported recently that SPR sensing can be enhanced based on nanomaterials which can modify the sensing substrate or be used as an amplification tag, which can enhance the electric field of the sensing substrate²⁸. With the improvement of the sensitivity, phase-sensitive SPR sensing can be used to monitor the interaction between proteins¹⁹ and detect specific molecules with extremely low concentration²⁹.

Methods

Theoretical Analysis. The Kretschmann configuration is used to optically excite SPR in our phase-sensitive SPR system. In the Kretschmann configuration, a 3 nm chromium layer and a 50 nm gold layer are deposited on a BK7 glass slide in sequence, which couples to the bevel of a coupling prism. When total internal reflection (TIR) occurs on the prism/gold interface, an evanescent wave is induced with the wave vector parallel to the interface as

$$k_{ev} = \frac{\omega}{c} n_p \sin \theta_i \quad (1)$$

where n_p represents the refractive index of the coupling prism, θ_i is the incident angle on the prism/gold interface, ω is the angular frequency of the incident light, and c is the speed of light. From Maxwell's equations, the propagation constant of the surface plasmons confined to the interface between the gold and the sample can be deduced as

$$k_{sp} = \frac{\omega}{c} \sqrt{\frac{\epsilon_{sample} \epsilon_{gold}}{\epsilon_{sample} + \epsilon_{gold}}} \quad (2)$$

where ϵ_{sample} and ϵ_{gold} are the dielectric constants of the sample and the gold, respectively.

When $k_{\text{ev}} = k_{\text{sp}}$, the surface plasmon can be resonantly excited. The reflected p-polarized light suffers a phase jump while the phase of the s-polarized light stays almost unchanged. As a result, a phase difference φ_{spr} is created, which is related to the refractive index of the sample in contact with the gold surface. In our system, a parallel-moving prism phase modulator (PM-PPM) is used to extract φ_{spr} . In the novel proposed PM-PPM, the phase difference between p-polarized and s-polarized light can be modulated by the TIR in an uncoated rhombic prism. It is apparent to all that TIR occurs on a prism/air interface when the light incident angle θ_i is larger than the critical angle, which will lead to a different phase shift of p-polarized light and s-polarized light. From the formula of the reflectivity of p-polarized and s-polarized light (i.e., the Fresnel formula), the phase difference φ_m after m times TIR can be calculated as follows^{30,31},

$$\varphi_m = \varphi_p - \varphi_s = 2m \tan^{-1} \left(\frac{\cos \theta_i \sqrt{n^2 \sin^2 \theta_i - 1}}{n \sin^2 \theta_i} \right) \quad (3)$$

where n represents the refractive index of the prism. φ_p and φ_s are defined as the phase shifts of p-polarized light and s-polarized light after m times (m counts) of TIR at the incident angle of θ_i . It is worth noting that φ_m is determined by the refractive index of the prism, the incident angle and the TIR count. When the refractive index of the prism and the TIR count are fixed, we can achieve different phase difference between p-polarized and s-polarized light by modulating the incident angle. The rhombic prism is quite suitable to be used as a phase difference modulator in phase-sensitive SPR biosensors because of the unique characteristics of the TIR.

The interference intensity between the projection of p-polarized and s-polarized can be described as,

$$I = I_p + I_s + 2\sqrt{I_p I_s} (\cos \varphi_{\text{spr}} + \varphi_m) \quad (4)$$

where I_p and I_s are the projection intensities of the reflected p-polarized and s-polarized light on the axis of the linear analyzer. By the expansion of the cosine component, the interference intensity can also be written as,

$$I = I_p + I_s + 2\sqrt{I_p I_s} \cos \varphi_{\text{spr}} \cos \varphi_m - 2\sqrt{I_p I_s} \sin \varphi_{\text{spr}} \sin \varphi_m \quad (5)$$

When $I_A = I_p + I_s$, $I_B = 2\sqrt{I_p I_s} \cos \varphi_{\text{spr}}$ and $I_C = 2\sqrt{I_p I_s} \sin \varphi_{\text{spr}}$, the interference intensity can be simplified to

$$I = I_A + I_B \cos \varphi_m - I_C \sin \varphi_m \quad (6)$$

The phase of SPR can be extracted by

$$\varphi_{\text{spr}} = \arctan \left(\frac{I_C}{I_B} \right) \quad (7)$$

Three different φ_{mi} ($i = 1, 2, 3$), i.e., $\varphi_{m1} = 0.85\pi$, $\varphi_{m2} = 0.66\pi$ and $\varphi_{m3} = 0.40\pi$ can be offered by PM-PPM with three prisms fixed on a motor-driven stage in different incident angles, and the related I_i ($i = 1, 2, 3$) can be detected correspondingly. The interference intensity can be written in the form

$$I_i = I_A + I_B \cos \varphi_{mi} - I_C \sin \varphi_{mi}, \quad i = 1, 2, 3 \quad (8)$$

As a result, the phase of SPR φ_{spr} can be extracted after I_B and I_C are calculated.

MF Exposure System. The ELF-MF exposure system (OX9-1) used in this study was designed and provided by Dr. Bao³². It consists of a “U” type magnet enwrapped in coils, a current amplifier, and a central regulator. Once initiated, ELF-MF (e.g., 50 Hz MF) was produced inside the magnet, and the central regulator was used to control the intensity and frequency. The control group was conducted under the same conditions but without the ELF-MF exposure.

Statistical Analysis. For each experiment, the value was presented as means \pm standard deviation (SD). All computations were performed with SPSS 16.0. The statistical differences between exposed and sham-exposed were tested using the Dunnett’s two-tailed t -test. A probability level of $P < 0.05$ was considered statistically significant.

References

1. Repacholi, M. Concern that “EMF” magnetic fields from power lines cause cancer. *Sci Total Environ* **426**, 454–458 (2012).
2. McNamee, D. A. *et al.* A literature review: the cardiovascular effects of exposure to extremely low frequency electromagnetic fields. *Int Arch Occup Environ Health* **82**, 919–933 (2009).
3. Lazzaro, D. V. *et al.* A consensus panel review of central nervous system effects of the exposure to low-intensity extremely low-frequency magnetic fields. *Brain Stimul* **6**, 469–476 (2013).
4. Vijayalaxmi & Prihoda, T. J. Genetic damage in mammalian somatic cells exposed to extremely low frequency electro-magnetic fields: a meta-analysis of data from 87 publications (1990–2007). *Int J Radiat Biol* **85**, 196–213 (2009).
5. Lee, H. C. *et al.* Effect of extremely low frequency magnetic fields on cell proliferation and gene expression. *Bioelectromagnetics* **36**, 506–516 (2015).
6. Wang, H. *et al.* Correlation between the dielectric properties and biological activities of human *ex vivo* hepatic tissue. *Phys Med Biol* **60**, 2603–2617 (2015).
7. Funk, R. H., Monsees, T. & Ozkucur, N. Electromagnetic effects - From cell biology to medicine. *Prog Histochem Cytochem* **43**, 177–264 (2009).

8. Halter, R. J., Hartov, A. & Paulsen, K. D. A broadband high-frequency electrical impedance tomography system for breast imaging. *IEEE Trans Biomed Eng* **55**, 650–659 (2008).
9. Laufer, S., Ivorra, A., Reuter, V. E., Rubinsky, B. & Solomon, S. B. Electrical impedance characterization of normal and cancerous human hepatic tissue. *Physiol Meas* **31**, 995–1009 (2010).
10. Nelson, S. G., Johnston, K. S. & Yee, S. S. High sensitivity surface plasmon resonance sensor based on phase detection. *Sens Actuators, B* **35**, 187–191 (1996).
11. Abdulhalim, I., Zourob, M. & Lakhtakia A. Surface plasmon resonance for biosensing: a mini-review. *Electromagnetics* **28**, 214–242 (2008).
12. Homola, J. Surface plasmon resonance sensors for detection of chemical and biological species. *Chem Rev* **108**, 462–493 (2008).
13. Schasfoort, R. B. & Ma, A. J. T. Handbook of Surface Plasmon Resonance. *Royal Society of Chemistry*, doi: 10.1039/9781847558220 (2008).
14. Majka, J. & Speck, C. Analysis of protein-DNA interactions using surface plasmon resonance. *Analytics of Protein-DNA Interactions* **104**, 13–36 (2007).
15. Teh, H. F., Peh, W. Y., Su, X. D. & Thomsen, J. S. Characterization of protein-DNA interactions using surface plasmon resonance spectroscopy with various assay schemes. *Biochemistry* **46**, 2127–2135 (2007).
16. Baron, O. L., Pauron, D. & Antipolis, S. Protein-lipid interaction analysis by surface plasmon resonance (SPR). *Bio-Protocol* **4**, 1–8 (2014).
17. Zijlstra, P., Paulo, P. M. & Orrit, M. Optical detection of single non-absorbing molecules using the surface plasmon resonance of a gold nanorod. *Nat Nanotechnol* **7**, 379–382 (2012).
18. Jin, W. *et al.* A DNA sensor based on surface plasmon resonance for apoptosis-associated genes detection. *Biosens Bioelectron* **24**, 1266–1269 (2009).
19. Law, W. C., Yong, K. T., Baev, A. & Prasad, P. N. Sensitivity improved surface plasmon resonance biosensor for cancer biomarker detection based on plasmonic enhancement. *ACS Nano* **5**, 4858–4864 (2011).
20. Goodrich, T. T., Lee, H. J. & Corn, R. M. Direct detection of genomic DNA by enzymatically amplified SPR imaging measurements of RNA microarrays. *J Am Chem Soc* **126**, 4086–4087 (2004).
21. Shumaker-Parry, J. S., Aebersold, R. & Campbell, C. T. Parallel, quantitative measurement of protein binding to a 120-element double-stranded DNA array in real time using surface plasmon resonance microscopy. *Anal Chem* **76**, 2071–2082 (2004).
22. Manuel, M., Vidal, B., Lopez, R., Alegret, S. & Chamorro, J. A. Determination of Probable Alcohol Yield in Musts by Means of an Spr Optical Sensor. *Sens Actuators, B* **11**, 455–459 (1993).
23. Liedberg, B. & Lundstrom, I. Principle of biosensing with an extended coupling matrix and surface plasmon resonance. *Sens Actuators, B* **11**, 63–72 (1993).
24. Jorgenson, R. & Yee, S. S. A fiber-optic chemical sensor based on surface plasmon resonance. *Sens Actuators, B* **12**, 213–220 (1993).
25. Wong, C. L. *et al.* Real-time protein biosensor arrays based on surface plasmon resonance differential phase imaging. *Biosens Bioelectron* **24**, 606–612 (2008).
26. Law, W. C. *et al.* Wide dynamic range phase-sensitive surface plasmon resonance biosensor based on measuring the modulation harmonics. *Biosens Bioelectron* **23**, 627–632 (2007).
27. Zeng, S. W. *et al.* Size dependence of Au NP-enhanced surface plasmon resonance based on differential phase measurement. *Sens Actuators, B* **176**, 1128–1133 (2013).
28. Zeng, S. W., Baillargeat, D., Ho, H. P. & Yong, K. T. Nanomaterials enhanced surface plasmon resonance for biological and chemical sensing application. *Chem. Soc. Rev.* **43**, 3246–3452 (2014).
29. Zeng, S. W. *et al.* Graphene-gold metasurface architectures for ultrasensitive plasmonic sensing. *Adv. Mater.* **27**, 6163–6169 (2015).
30. Ye, G. A., Yang, W., Jiang, L. & He, S. L. Surface Plasmon Resonance Phase-Sensitive Imaging (SPR-PI) Sensor Based on a Novel Prism Phase Modulator. *PIER* **145**, 309–318 (2014).
31. Ye, G. A., Yang, W., Jiang, L., Qian, J. & He, S. L. A novel phase-sensitive SPR biosensor array based on prism phase modulator. *Smart Photonic and Optoelectronic Integrated Circuits Xvi* **8989** (2014).
32. Wang, S., Bao, J. L. & Zhu, C. Y. Development of Real-time Electromagnetic Field Exposure System for Cell. *High Voltage Engineering* **41**, 1409–1416 (2015).

Acknowledgements

We are grateful to Dr. Jiali Bao for assistance on the ELF-MF exposure system. This study was supported by grants from the Ministry of Science and Technology (2011CB503702), the Science and Technology Department of Zhejiang Province (2010R50007) and the National Natural Science Foundation of China (81573109).

Author Contributions

L.J. and X.Z. generated the experimental idea. L.J. set up the SPR system and completed the optical experiments. J.T. used the abbe refractometer to measure the refractive index. X.Z. analyzed the statistics. L.J., X.Z., Y.F. and D.Y. contributed in writing manuscript text. J.Q., G.C. and S.H. discussed the design of the structure and experimental results, as well as contributed in manuscript revise. S.H. finalized the manuscript.

Additional Information

Supplementary information accompanies this paper at <http://www.nature.com/srep>

Competing financial interests: The authors declare no competing financial interests.

How to cite this article: Jiang, L. *et al.* The effects of magnetic fields exposure on relative permittivity of saline solutions measured by a high resolution SPR system. *Sci. Rep.* **6**, 25111; doi: 10.1038/srep25111 (2016).



This work is licensed under a Creative Commons Attribution 4.0 International License. The images or other third party material in this article are included in the article's Creative Commons license, unless indicated otherwise in the credit line; if the material is not included under the Creative Commons license, users will need to obtain permission from the license holder to reproduce the material. To view a copy of this license, visit <http://creativecommons.org/licenses/by/4.0/>